Silver nanoclusters-assisted triple-amplified biosensor for ultrasensitive methyltransferase activity detection based on AuNPs/ERGO hybrids and hybridization chain reaction

Xiaolun Peng, Jinlin Zhu, Wei Wen, Ting Bao, Xiuhua Zhang, Hanping He, Shengfu Wang

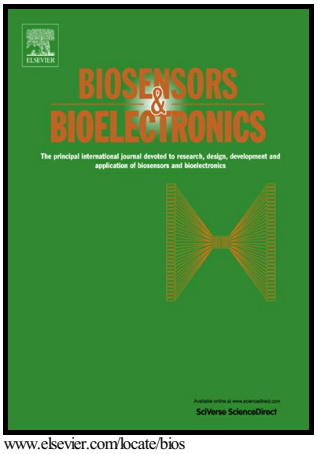

www.elsevier.com/locate/bios

PII: S0956-5663(18)30551-7
DOI: https://doi.org/10.1016/j.bios.2018.07.048
Reference: BIOS10637

To appear in: *Biosensors and Bioelectronic*

Received date: 5 May 2018
Revised date: 25 July 2018
Accepted date: 25 July 2018

Cite this article as: Xiaolun Peng, Jinlin Zhu, Wei Wen, Ting Bao, Xiuhua Zhang, Hanping He and Shengfu Wang, Silver nanoclusters-assisted triple-amplified biosensor for ultrasensitive methyltransferase activity detection based on AuNPs/ERGO hybrids and hybridization chain reaction, *Biosensors and Bioelectronic,* https://doi.org/10.1016/j.bios.2018.07.048

Silver nanoclusters-assisted triple-amplified biosensor for ultrasensitive methyltransferase activity detection based on AuNPs/ERGO hybrids and hybridization chain reaction

Xiaolun Peng, Jinlin Zhu, Wei Wen, Ting Bao, Xiuhua Zhang, Hanping He, Shengfu Wang*

Hubei Collaborative Innovation Center for Advanced Organic Chemical Materials, Ministry of Education Key Laboratory for the Synthesis and Application of Organic Functional Molecules & College of Chemistry and Chemical Engineering, Hubei University, Wuhan 430062, PR China

*Corresponding author. Telephone: +86-27-50865309; Fax: +86-27-88663043; E-mail address: wangsf@hubu.edu.cn.

Abstract

In the paper, a triple-amplified biosensor was built for the purpose of ultrasensitive methyltransferase (Dam MTase) activity detection and inhibitor screening based on in-situ synthesized silver nanoclusters (AgNCs) as signal probes to provide amplified current signal coupling with gold nanoparticles/electrochemical reduced graphene oxide (AuNPs/ERGO) hybrids and hybridization chain reactions (HCR) amplification strategy. For biosensor preparation, the AuNPs/ERGO hybrids were firstly generated on the electrode surface by electrochemical co-reduction method, then the ds-DNA structures which comprised the specific recognition sequences (5'-G-A-T-C-3') of the Dam MTase and the restrictive endonuclease DpnI were formed on the electrode by the hybridization of the assistant DNA with the capture DNA. The presence of Dam MTase methylated partial ds-DNA structures on the electrode which could be digested by DpnI and could not undergo HCR process. The unmethylated ds-DNA structures underwent HCR process to further hybridize with DNA1 and DNA2 to form ds-DNA superstructures as effective template for AgNCs in-situ synthesis. Oxidation peak current of silver was obtained as signal output for Dam MTase detection. Integrated synthesis and detection in

one as well as combined metal nanocluster with DNA superstructures, this biosensor showed a good performance for Dam MTase activity detection with a detection limit of 0.0073 U/mL. Compared with reported biosensor, the designed biosensor showed high sensitivity and had potential in clinical diagnosis as well as inhibitor screening.

Graphical Abstract:

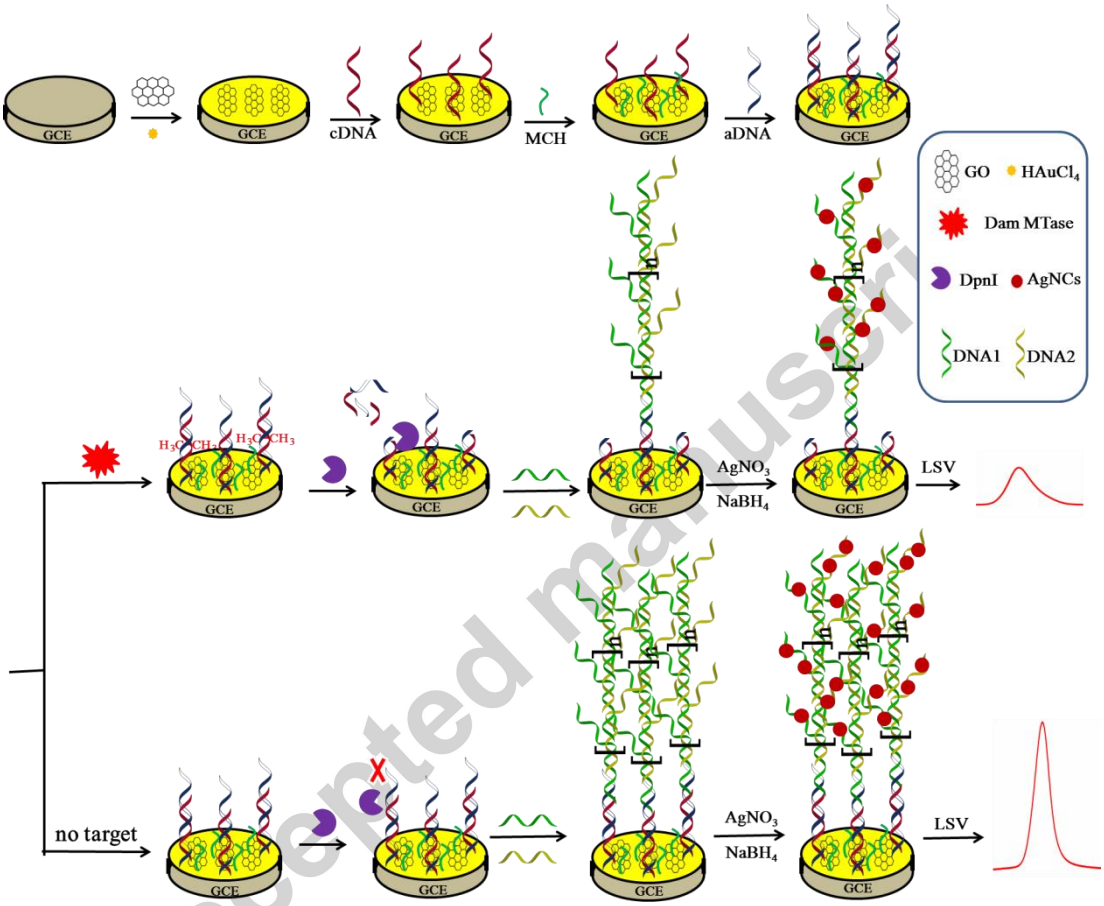

Keywords

Electrochemical biosensor; Methyltransferase activity; Hybridization chain reactions; Silver nanoclusters; Clinical diagnosis; Inhibitor screening.

1. Introduction

DNA methylation is a vital long-term gene silencing mechanism and involves in gene regulation (Muren and Barton, 2013), which is usually assisted by DNA methyltransferases (MTase) (Cheng and Roberts, 2001). DNA methylation is closely bound up with many biological processes including X chromosome passivation, regulation of gene expression, and transposon silencing (Jeltsch et al., 2002; Jones and Miranda, 2007). Both hypermethylation and demethylation have brought about various tumor types (Baylin et al., 1998; Das et al., 2004). Many studies have shown that abnormal expression of DNA MTase is tightly attached to various diseases and bacterial infections (Erova et al., 2006), thus DNA MTase has immense latent energy in anticancer treatment and drug screening (Mutze et al., 2011; Singh et al., 2013), especially in early diagnosis of tumors (Das and Singal, 2004). The aberrant DNA MTase activity could be as latent markers for early diagnosis of cancer and other diseases (Konno et al., 2004; Esteller et al., 1999). Therefore, constructing an innovation to achieve effective detection of DNA MTase activity has far-reaching significance and lays the foundation for clinical diagnosis.

In these years, various assays have already been developed for DNA MTase detection including radioactive labeling (Pradhan et al., 1995), HPLC (Friso et al., 2002), surface plasma resonance techniques (Li et al., 2018), mass spectrometry (Huang et al., 2016), fluorescence (Gao et al., 2014) and electrochemistry (Wang et al., 2015； Liu et al., 2016; Wu et al., 2012). Compared with other methods, electrochemical method has remarkable superiorities including simple operation, inexpensive instrument, fast response, high sensitivity, thus has been far and wide applied into detecting various biological substances. In typical electrochemical assay for DNA MTase, DNA hybrids or antibody complex fixed on the electrode are generally modified with

electroactive molecules or used to absorb electroactive molecules (such as ferrocene, methylene blue), which can be used as a signal probe. For instance, Liu et al. successfully achieved the quantitative assay of DNA MTase by means of ferrocene as signal probe (Liu et al., 2011). Jing et al. synthesized DNA-AuNPs signal amplification unit to adsorb methylene blue for highly sensitive DNA methylation measurement (Jing et al., 2014). However, despite some improved performance, the detection sensitivity and probe activity are unsatisfactory. In order to magnify the current response, numerous signal amplification approaches have been adopted including enzyme catalytic reaction (Gao et al., 2014; Huang et al., 2014), nuclease-assisted multiple amplification strategy (Liu et al., 2013a, 2013b; Jie et al., 2017), hybridization chain reaction (HCR) (Bao et al., 2015; Zhang et al., 2012). In addition, these amplification approaches are often used in conjunction with some nanomaterials due to their good properties (Zeng et al., 2010; Dong et al., 2012; Hu et al., 2014). HCR is one of the most attractive enzyme-free amplification methods, in which DNA is used as structural material to form superstructures through self-assembly to improve signal output, and has been applied in construction of electrochemical biosensor for inorganic ion and biomolecule detection. The use of HCR in combination with some excellent new nanomaterials will certainly have surprising sensing performance.

Metal nanoclusters (MNCs) have smaller size than metal nanoparticles and hold numerous unique properties including good conductivity, biocompatibility, large specific surface area, easy modification (Wilcoxon and Abrams, 2006). Due to wonderful intrinsic fluorescence property, MNCs have potential as fluorescent probes for bioimaging application (Zhang and Wang, 2014). The good conductivity and large specific surface area can improve sensitivity when constructing electrochemical biosensor and the aptamer/antibody can be fixed on the electrode through the

interaction with MNCs, thus their application in electrochemistry has caused widespread concern in recent years (Guo and Wang, 2011). For example, our group synthesized functionalized gold nanoclusters/graphene nanohybrids for DNA detection (Wang et al., 2017). In addition, some metal nanoclusters themselves have redox signals (e.g. AuNCs, AgNCs, CuNCs) and can be directly used as signal probes for target detection, avoiding some modification steps (Wang et al., 2017; Dong et al., 2012; Jie et al, 2017). Recently, DNA-stabilized AgNCs has been reported as multifunctional biolabels for electrochemical analysis, but most of these preparation processes are time-consuming and fussy. To improve preparation efficiency and maintain probe stability, in-situ generation of silver nanoclusters using DNA superstructures formed by HCR as a template is more effective than ex-situ preparation, at the same time, it also simplifies the following fixing steps. Synthesis and detection integration greatly ensure the activity of the probe, and at the same time incorporate multiple amplification strategies to increase the detection sensitivity.

Based on the above discussion, we constructed a triple-amplified electrochemical biosensor, using in-situ synthesized AgNCs as signal probes, combined with AuNPs/ERGO hybrids and HCR amplification strategy for ultrasensitive detection of DNA MTase. The AuNPs/ERGO hybrids were in-situ generated on the surface of the glassy carbon electrode (GCE) by a green and lowcost electrochemical co-reduction method which could be an effective load platform to assemble more capture DNA and increased the conductivity and the surface area of the electrode. HCR caused by the continuous hybridization of DNA not only amplified the signal but also provided a large number of templates for AgNCs synthesis. The generated AgNCs produced continuous and stable current output by virtue of their own redox properties, without the need to add additional electroactive molecules. Integrated synthesis and detection in one as well as combined metal

nanocluster with DNA superstructures, this triple-amplified biosensor showed admirable sensitivity and selectivity for Dam MTase activity assay.

2. Experimental Sections

2.1 Reagents and materials

DNA adenine methylation methyltransferase (Dam MTase), CpG methyltransferase (M.SssI MTase), S-Adenosylmethionine (SAM), restriction endonucleases DpnI (DpnI) and restriction endonucleases HpaII (HpaII) were received from New England Biolabs Inc (Beijing, China). Silver nitrate ($AgNO_3$), 6-mercapto-1-hexanol (MCH) and Gold (III) chloride trihydrate ($HAuCl_4 \cdot 3H_2O$) were purchased from Sigma-Aldrich (USA). Tris (2-carboxyethyl) phosphine hydrochloride (TCEP), albumin from bovine serum (BSA) and sodium borohydride ($NaBH_4$) were purchased from Aladdin Bio-Chem Technology Co., Ltd. (Shanghai, China). Graphene oxide aqueous solution was got from Shanxi Institute of Coal Chemistry, Chinese Academy of Sciences. 20 mM Tris-HCl (pH 7.4) made up of 140 mM NaCl and 5 mM $MgCl_2$ was employed to prepare different concentrations of aptamer solution. In this experiment, all solutions were prepared using ultrapure water (resistivity of 18.25 MΩ cm) produced from Aquapro water purification system.

Oligonucleotides in this experiment were purchased from Sangon Biotech Co., Ltd. (Shanghai, China). Oligonucleotides sequence information was listed below:

Capture DNA (cDNA): 5'-SH-$(CH_2)_6$-GCTGAGATCTTTGCT-3'

Assistant DNA (aDNA): 5'-AAGGCATTGAAGCAAAGATCTCAGC-3'

DNA1: 5'-TCAATGCCTTAATCGAACGTCCCCCCCCCCC-3'

DNA2: 5'-CCCCCCCCCCCCAAGGCATTGAACGTTCGATT-3'

2.2 Apparatus

X-ray photoelectron spectroscopy (XPS) measurements were performed on a JSM6510LV instrument (Jeol, Japan). Scanning electron micrographs (SEM) were measured on a JEOL JSM7100F scanning electron microscope (Jeol, Japan). Transmission electron microscopy (TEM) images were given by the JEM-2100 transmission electron microscope (Japan). Fluorescence spectra were obtained from RF-5301PC spectrophotometer (Shimadzu Co., Japan). All electrochemical experiments including electrochemical impedance spectroscopic (EIS) and the linear sweep voltammetry (LSV) were measured with CHI 660E electrochemical workstation (CH Ins., Shanghai, China). A typical three-electrode system including a platinum electrode as auxiliary electrode, a GCE as working electrode and a saturated calomel electrode (SCE) as reference electrode was applied into this experiment. EIS was conducted in $[Fe(CN)_6]^{3-/4-}$ probe solution including 0.1 M KCl with a varying frequency from 0.1 to 10^5 Hz.

2.3 Fabrication of AuNPs/ERGO hybrids

The AuNPs/ERGO hybrids were prepared by the reported electrochemical co-reduction method with a slight modification (Yue et al, 2015). Firstly, the 1 mg/mL graphene oxide (GO) aqueous solution and the 1% chloroauric acid solution ($HAuCl_4$) were mixed to form a homogeneous solution and the final concentration of graphene oxide in the mixture was 0.25 mg/mL. Earlier to modification, the bare GCE was polished by γ-Al_2O_3 powder and treated by ultrasound with water and ethanol separately to remove the adsorbate, and then cyclic voltammetry (CV) was adopted to test the usability of the electrode. When the electrode was available, 10 μL prepared GO-$HAuCl_4$ mixture was dripped onto the surface of the electrode with a pipette and then dried in a thermostatic chamber for 30 min to form GO-$HAuCl_4$ membrane for further use. The AuNPs/ERGO/GCE was fabricated by electrochemical co-reducing the GO-$HAuCl_4$ membrane on the GCE surface. Specifically, GO-$HAuCl_4$

membrane /GCE as working electrode was immersed into the base solution of 0.1 M PBS (pH 7.0) to perform a CV scan with 10 laps and scan voltage ranged from 0 to -1.5 V at a scan rate of 50 mV/s. After that, the well-prepared electrode was used to construct the biosensor.

2.4 Construction of the designed biosensor

Primarily, 10 μL cDNA (1 μM) was dropped on the well-prepared modified electrode at room temperature for 12 h, and then treated by 10 μL MCH (1 mM) for 60 min. After rinsing with ultrapure water, 10 μL aDNA (1 μM) was added to hybridize with the cDNA on the modified electrode forming ds-DNA structure at 37 ℃ constant temperature incubator for 60 min. Subsequently, the electrode was incubated with 50 μL Dam MTase solution which was made of diverse concentration of Dam MTase and 320 μM SAM to carry out the methylation of ds-DNA structure at 37 ℃ for 60 min and 10 μL restrictive endonuclease DpnI (80 U/mL) was dropped on the electrode surface to specifically digest the methylated ds-DNA structures at 37 ℃ for 60 min in the next step. Since then, the electrode was bathed with plenty of ultrapure water to take away nonspecific adsorption. Finally, the electrode was incubated with the freshly prepared mixed solution of DNA1 and DNA2 (final concentration 2 μM) to further hybridize to build long ds-DNA superstructures at 37 ℃ for 70 min.

2.5 In-situ synthesis of silver nanoclusters on electrode

The successfully formed long ds-DNA superstructures on the electrode could be used as an effective template for synthesizing AgNCs. The synthetic steps referred to the literature with mild revamps (Jie et al, 2017). For the details, 10 μL $AgNO_3$ (200 μM) was added on the electrode and incubated in the dark for 30 min, and then 8 μL freshly prepared $NaBH_4$ (500 μM) solution was applied to the electrode at once for the formation of AgNCs in the dark for another 120 min. After incubation, a mass of AgNCs were produced on the long ds-DNA superstructures.

2.6 Electrochemical measurement of the constructed biosensor

Linear sweep voltammetry (LSV) technique was used to record the signal output. Measurement was processed in 1 M KCl solution with three-electrode system, scanning from -0.1 V to +0.3 V with a scan rate of 100 mV/s. The oxidation current output of AgNCs occurred at about +0.05 V.

3 Results and discussion

3.1 Principle description of designed biosensor for Dam MTase activity assay

The triple-amplified biosensor was built based on in-situ generated silver nanoclusters as a signal probe to provide amplified current signal, integrated with electrochemically co-reduced AuNPs/ERGO hybrids and HCR amplification process. As mentioned in Scheme 1, the mixed solution of $HAuCl_4$ and GO was electrochemically reduced by CV scan on the surface of cleaned GCE to form AuNPs/ERGO hybrids membrane which immensely enlarged the superficial area and conductivity of the electrode. After that, cDNA bound to the electrode surface via self-assembly by means of the Au-S bond. MCH was used to sealed the redundant active sites and prevent nonspecific adsorption. The ds-DNA structures formed by the hybridization of the cDNA with the part of aDNA had a specific recognition sequence (5'-G-A-T-C-3') for both Dam MTase and DpnI. In the presence of Dam MTase, the Dam MTase transferred the methyl group of the SAM into the ds-DNA structures and methylated them while the DpnI could digest the methylated ds-DNA structures. The remaining part of aDNA in the unmethylated ds-DNA structures hybridized with DNA1, at the same time, the continuous hybridization of DNA1 and DNA2 triggered HCR process to produce ds-DNA superstructures. As the target concentration increased, the resulting ds-DNA superstructures decreased. In the absence of Dam MTase, no ds-DNA structures were methylated and digested. After adding some DNA1 and DNA2, maximum ds-DNA superstructures were produced. The terminal parts of DNA1 and DNA2 which

contained cytosine-rich sequences could be as effective template for AgNCs synthesis. The abundant AgNCs could be in-situ generated on the ds-DNA superstructures of the electrode with the $AgNO_3$ and $NaBH_4$. The content of Dam MTase could be precisely detected according to the correlativity between the concentration of Dam MTase and signal output. Moreover, the triple-amplified strategy highly improved the sensitivity of the proposed biosensor.

3.2 Characterization of the modification steps of the biosensor and the nanomaterials

EIS and LSV were used to characterize the construction process of biosensor. As shown in Fig. 1A, the diameter of the semicircle in EIS was equal to electron transfer resistance (R_{et}). Inset showed the equivalent circuit of EIS, from which the value of impedance could be theoretically simulated. The R_{et} of bare GCE (curve a) was 1972 Ω through impedance simulation. The R_{et} greatly reduced to 709 Ω after the formation of the AuNPs/ERGO hybrids on the electrode surface (curve b), indicating that electron transfer rate was immensely accelerated. As the cDNA (curve c) and MCH (curve d) were modified on the GCE, the R_{et} raised significantly. When the ds-DNA structures were formed on the GCE, the R_{et} increased to 8776 Ω (curve e). This might be due to the negative charges of the oligonucleotides had electrostatic repulsion to $[Fe(CN)_6]^{3-/4-}$ probe. After the GCE was treated with Dam MTase and DpnI, the R_{et} decreased to 3324 Ω (curve f), which demonstrated that the methylated ds-DNA structures were digested by DpnI. With the addition of DNA1 and DNA2, the R_{et} increased dramatically to 13420 Ω (curve g) due to HCR process. In-situ generated AgNCs decreased the R_{et} to 7492 Ω (curve h) again because of their good conductivity. The good performance of EIS suggested the biosensor was successfully built. The LSV was used to prove the feasibility of biosensor (Fig. 1B). The initial current response was very high without Dam MTase (curve a), showing that DpnI could not digest unmethylated ds-DNA structures and could generate a large number of AgNCs through HCR

process. Similarly, at the existence of Dam MTase, methylated ds-DNA structures were retained without DpnI (curve b). The current signal dropped significantly after the GCE was incubated with Dam MTase (1 U/mL) and DpnI (curve c) because partial ds-DNA structures were digested and could not generate AgNCs in-situ. Without addition of DNA1 and DNA2 into the system, HCR could not be successfully triggered to generate effective template for AgNCs synthesis, so the current signal was very low (curve d). The above phenomenon proved the rationality of the designed biosensor.

The SEM and XPS characterization were used to prove the formation of AuNPs/ERGO hybrids (See related description in Supporting Information). To further investigate the morphology and optical properties of AgNCs, TEM characterization and fluorescence spectrum characterization were carried out in our experiment. As shown in Fig. 2A, AgNCs was well-dispersed on the whole, spherical in morphology with average diameters about 4 nm. It could be seen from Fig. 2B that the generated AgNCs had good fluorescence characteristics. Before adding $AgNO_3$ and $NaBH_4$, the ds-DNA structures showed no fluorescence peak; after adding $AgNO_3$ and $NaBH_4$ and incubated with ds-DNA structures for 120 min, an obvious fluorescence emission peak was observed at 600 nm with an excitation peak at 561 nm, which was consistent with the reported results. (Tao et al., 2012).

3.3 Optimization of experimental conditions

The DpnI digestion procedure and HCR process played an important role in constructing biosensor, therefore the DpnI digestion time and HCR time were investigated in Fig. S3. As shown in Fig. S3A, the digestion level was bound up with the digestion time, so the GCE was treated with DpnI for changed time after incubated with Dam MTase and recorded current signal. At the beginning, the digestion level of DpnI obviously improved with the digestion time increasing, so the current signal was drastically declining. After a period of time, the digestion level eventually reaching a plateau, and

hence 60 min was considered to be the optimum digestion time and was chosen for the experiment. Fig. S3B studied the impact of HCR time on the system while the other experimental conditions were controlled. The electrode firstly was incubated with Dam MTase (1 U/mL) and DpnI, and then incubated with DNA1 and DNA2 for different time. The current output of AgNCs was read-in. As time increased, the current firstly increased and stayed stable after reaching a plateau at 70 min, so the 70 min was selected as optimal HCR time for the system (optimization of the volume ratio of $HAuCl_4$ and GO solution (Fig. S4) and the concentration and deposition time of $AgNO_3$ (Fig. S5) were shown in supporting information).

3.4 Current response of the constructed biosensor

The biosensor detection condition for Dam MTase was presented in Fig. 3. The ds-DNA structures were first formed on the modified electrode and later went through methylation process with a series of concentrations of Dam MTase. The unmethylated ds-DNA structures produced ds-DNA superstructures by the HCR process as a template to in-situ generate AgNCs. The LSV responses of AgNCs were presented in Fig. 3A, which revealed that as the concentration of Dam MTase increased, the current response signal decreased. Because the more Dam MTase there was, the more methylated ds-DNA there were, and the less ds-DNA structures were left on the electrodes after digestion, which led to the less AgNCs generated after HCR process. The linear relationship between the current responses and the logarithm of Dam MTase concentration with concentration range from 0.02 U/mL to 10 U/mL was presented in Fig. 3B. The obtained linear equation was $I = 1.61 - 1.38 \log c$ ($R^2 = 0.9984$) and the limit of detection (LOD) was calculated as 0.0073 U/mL ($3\sigma/k$). Compared with other methods for Dam MTase detection (Table 1), this triple-amplified biosensor not only integrated the amplification advantages of HCR and AgNCs but also the in-situ preparation process was high-efficiency, thus

showed a wider linear range and a lower detection limit and could better achieve the ultrasensitive detection of the target.

3.5 Selectivity of the constructed biosensor

To better discuss the superiority about designed biosensor, the selectivity of the biosensor was discussed in Fig. 4A. Three interfering substances (M.SssI MTase, HpaII and BSA) were picked and their concentration was 1 U/mL, 1 U/mL and 1%, respectively. For lack of target (Blank), no ds-DNA structures were digested, thus exhibiting a high current signal. With Dam MTase increasing, the current signal drops drastically to less than a third of the original, indicating that the partially methylated ds-DNA structures were digested. Nevertheless, 1 U/mL HpaII almost had the same current response with the blank, at the same time, 1 U/mL M.SssI MTase and 1% BSA made the signal slightly decreased. Therefore, the constructed biosensor exhibited relatively good selectivity for Dam MTase detection. In addition, the repeatability of the biosensor was also presented in Fig S6. At the same experimental conditions, eight modified electrodes were used to test the repeatability of the biosensor. Eight electrodes had similar LSV current signal and the RSD was about 1%, which showed good repeatability of the constructed biosensor.

3.6 Detection in serum samples

For purpose of exploring the potential of prepared biosensor in practical application, Dam MTase was detected in 100-fold diluted serum samples for recovery experiments (Table S1). Three disparate concentrations of Dam MTase (0.1 U/mL, 1 U/mL, 10 U/mL) prepared with diluted serum samples were measured. By calculation, the recovery rate was between 92.5% and 97.9% and the RSD was between 1.07% and 2.49%, which demonstated that the constructed biosensor could achieve accurate determination of the Dam MTase in complex biological samples.

3.7 Influence of different inhibitors on Dam MTase activity

Dam MTase activity played a key role in the methylation process, so the biological inhibitors had important value in drug screening. In order to investigate the feasibility of the proposed biosensor in the DNA MTase inhibitors screening, gentamycin and 5-fluorouracil were chosen as the model inhibitors to be thoroughly investigated. Fig. 4B showed the relative activity of Dam MTase decreased with the concentration of 5-fluorouracil increasing and then nearly reached a platform. Only half of the Dam MTase activity remained when the 5-fluorouracil was at 100 μM. By contrast with 5-fluorouracil, the gentamycin evidently put up more distinct inhibition on Dam MTase activity, which caused 50% inhibition at 1 μM (Fig. 4C). These results were in accordance with the literature (Wang et al., 2013) and reflected the proposed biosensor possessed promising application in Dam MTase inhibitor screening.

4 Conclusion

In summary, we developed a triple-amplified electrochemical biosensor for highly sensitive and selective Dam MTase activity detection based on AuNPs/ERGO hybrids and HCR amplification strategy, using in-situ generated AgNCs as signal probe. In our designs, The AuNPs/ERGO hybrids as load platform were formed by a green and lowcost electrochemical co-reduction method. The Dam MTase could methylate partial ds-DNA structures which were subsequently digested by DpnI. The ds-DNA structures after being digested could not undergoing HCR process so that ds-DNA superstructures could not be produced to in-situ generate AgNCs, leading a decrease in signal. Introducing multiple amplification strategy ensured the high sensitivity of DNA MTase assay. In contrast to the reported methods, the constructed biosensor was sensitive with a detection limit low to 0.0073 U/mL. Importantly, the designed biosensor showed good performance in serum samples and

inhibitor screening, having great potential in clinical diagnosis as well as drug discovery.

Acknowledgments

This work was supported by the National Natural Science Foundation of China (Grant No. 21475032).

Appendix A. Supporting information

Supplementary information related to this paper can be discovered in the online version, at

Reference

Bao, T., Wen, W., Zhang, X.H., Xia, Q.H., Wang, S.F., 2015. Biosens. Bioelectron. 70, 318–323.

Baylin, S.B., Herman, J.G., Graff, J.R., Vertino, P.M., Issa, J.P., 1998. Adv. Cancer Res. 72, 141-196.

Cheng, X., Roberts, R.J., 2001. Nucleic Acids Research. 29, 3784–3795.

Dong, H.F., Jin, S., Ju, H.X., Hao, K.H., Xu, L.P., Lu, H.T., Zhang, X.J., 2012. Anal. Chem. 84(20), 8670-8674.

Dong, H.F., Zhang, J., Ju, H.X., Lu, H.T., Wang, S.Y., Jin, S., Hao, K.H., Du, H.W., Zhang, X.J., 2012. Anal. Chem. 84(10), 4587-4593.

Erova, T.E., Pillai, L., Fadl, A.A., Sha, J., Wang, S.F., Galindo, C.L., Chopra, A.K., 2006. Infection and Immunity 74, 410–424.

Esteller, M., Hamilton, S.R., Burger, P.C., Baylin, S.B., Herman, J.G., 1999. Cancer Res. 59, 793–797.

Friso, S., Choi, S., Dolnikowski, G.G., Selhub, J., 2002. Anal. Chem. 74, 4526-4531.

Gao, C.Y., Li, H.N., Liu, Y.J., Wei, W., Zhang, Y.J., Liu, S.Q., 2014. Analyst 139, 6387–6392.

Gao, Z.Q., Hou, L., Xu, M.D., Tang, D.P., 2014. Scientific Reports 4, 3966.

Guo, S.J., Wang, E.K., 2011. Nantod. 6, 240-264.

Huang, J.H., Gao, X., Jia, J.J., Kim, J.K., Li, Z.G., 2014. Anal. Chem. 86, 3209–3215.

Huang, W., Qi, C.B., Lv, S.W., Xie, M., Feng, Y.Q., Huang, W.H., Yuan, B.F., 2016. Anal. Chem. 88(2), 1378-1384.

Hu, R., Wen, W., Wang, Q.L., Xiong, H.Y., Zhang, X.H., Gu, H.S., Wang, S.F., 2014. Biosens. Bioelectron. 53, 384-389.

Jeltsch, A., 2002. ChemBioChem. 3, 274-293.

Jie, G.F., Lu, Z.K., Zhao, Y., Wang, X.C., 2017. Sens. Actuators B. 240, 857–862.

Jie, G.F., Tan, L., Zhao, Y., Wang, X.C., 2017. Biosens. Bioelectron. 94, 243–249.

Jing, X.Y., Cao, X.Q., Wang, L., Lan, T., Li, Y.Y., Xie, G.M., 2014. Biosens. Bioelectron. 58, 40–47.

Jones, P.A., Miranda, T.B., 2007. J. Cell. Physiol. 213, 384-390.

Konno, S., Morishita, Y., Fukasawa, M., Shu, Y., Wang, D., Tanaka, R., Minami, Y., Iijima, T., Noguchi, M., 2004. Cancer Cytopathol 102, 348–354.

Liu, P., Wang, D.D., Zhou, Y L., Wang, H. Y., Yin, H.S., Ai, S.Y., 2016. Biosens.Bioelectron. 80, 74-78.

Liu, S.F., Wang, C.F., Zhang, C.X., Wang, Y., Tang, B., 2013a. Anal. Chem. 85, 2282–2288.

Liu, X., Wang, F., Aizen, R., Yehezkeli, O., Willner, I., 2013b. J. Am. Chem. Soc. 135, 11832–11839.

Li, W., Hou, T., Wu, M., Li, F., 2016. Talanta. 148, 116-121.

Li, Z.M., Zhang, X., Liang, R.P., Zheng, X.J., Qiu, J.D., 2018. Anal. Chim. Acta 1016, 12-18.

Mardiak, J., Salek, T., Sycova-Mila, Z., Hlavata, Z., Obertova, J., Mego, M., Reckova, M., Koza, I., 2004. J. Clin. Oncol 22, 4632-4642.

Muren, N.B., Barton, J.K., 2013. J. Am. Chem. Soc. 135, 16632-16640.

Mutze, K., Langer, R., Schumacher, F., Becker, K., Ott, K., Novotny, A., Hapfelmeier, A., Höfler, A., Keller, G., 2001. Eur. J. Cancer 47, 1817–1825.

Peng, X.L., Hu, T.X., Bao, T., Zhao, L., Zeng, X., Wen, W., Zhang, X.H., Wang, S.F. 2017. Journal of Electroanalytical Chemistry. 799, 327-332.

Pradhan, S., Bacolla, A., Wells, R.D., Roberts, R.J., 1995. J. Biol. Chem. 274, 33002-33010.

Singh, V., Sharma, P., Capalash, N., 2013. Cancer Drug Targets 13, 379–399.

Tao, Y., Lin, Y.H., Huang, Z.Z., Ren, J.S., Qu, X.G., 2012. Analyst.137, 2588–2592.

Wang, Q., Pan, M., Wei, J., Liu, X.Q., Wang, F. 2017. ACS Sens. 2, 932-939.

Wang,W., Bao, T., Zeng, X., Xiong, H.Y., Wen, W., Zhang, X.H., Wang, S.F., 2017. Biosens.Bioelectron. 91, 183–189.

Wang, X.Z., Liu, X.L., Hou, T., Li, W., Li, F., 2015. Sens. Actuators B. 208(0), 575–580.

Wang, Y.J., Zhang, X.Y., Zhao, L., Bao, T., Wen, W., Zhang, X.H., Wang, S.F., 2017. Biosens. Bioelectron. 98, 386–391.

Wenzel, C., Guschlbauer, W., 1993. Nucleic Acids Res. 21, 4604–4609.

Wilcoxon, J.P., Abrams, B.L., 2006. Chem. Soc. Rev. 35, 1162–1194.

Wu, H.W., Liu, S.C., Jiang, J.H., Shen, G.L., Yu, R.Q., 2012. Chem. Commun. 48, 6280-6282.

Xing, X.W., Tang, F., Wu, J., Chu, J.M., Feng, Y.Q., Zhou, X., Yuan, B.F. 2014. Anal. Chem. 86, 11269-11274.

Yue, X.Y., Song, W.S., Zhu, W.X., Wang, J.L., Wang, Y.R., 2015. Electrochimica Acta 182, 847–855.

Zeng, Q., Cheng, J.S., Tang, L.H., Liu, X.F., Liu, Y.Z., Li, J.H., Jiang, J.H., 2010. Adv. Funct. Mater. 20(19), 3366-3372.

Zhang, B., Liu, B.Q., Tang, D.P., Niessner, R., Chen, G.N., Knopp, D., 2012. Anal. Chem. 84(12), 5392-5399.

Zhang, H., Dong, H.L., Yang, G.Q., Chen, H.F., Cai, C.X., 2016. Anal. Chem. 88(22), 11108-11114.

Zhang, L.B., Wang, E.K., 2014. Nantod. 9(1), 132-157.

Zhao, H.F., Liang, R.P., Wang, J.W., Qiu, J.D. 2015. Biosens.Bioelectron. 63, 458-464.

Zhou, X.Y., Zhao, M., Duan, X.L., Guo, B., Cheng, W., Ding, S.J., Ju, H.G. 2017. ACS Appl. Mater. Interfaces. 9(46), 40087-40093.

Scheme 1. Schematic Illustration of designed electrochemical biosensor for Dam MTase activity detection.

Fig. 1. (A) EIS plots of the biosensor: (a) bare GCE; (b) AuNPs/ERGO hybrids/GCE; (c) cDNA/AuNPs/ERGO hybrids/GCE; (d) MCH/cDNA/AuNPs/ERGO hybrids/GCE; (e) aDNA/MCH/cDNA/AuNPs/ERGO hybrids/GCE; (f) after aDNA/MCH/cDNA/AuNPs/ERGO hybrids/GCE incubated with Dam MTase and DpnI; (g) DNA1/DNA2/aDNA/MCH/cDNA/AuNPs/ERGO hybrids/GCE; (h) after in-situ synthesized AgNCs. (B) LSV response of the biosensor: (a) the biosensor without Dam MTase; (b) without DpnI; (c) incubated with 1 U/mL Dam MTase and 80 U/mL DpnI; (d) without HCR strategy.

Fig. 2. (A) TEM images of in-situ synthesized AgNCs. (B) The Fluorescence spectrum of the preparation process of AgNCs after (a) and before (b) adding $AgNO_3$ and $NaBH_4$ into ds-DNA superstructures.

Fig. 3. (A) LSV responses corresponding to different concentrations of target under optimized condition: (a) 0, (b) 0.02 U/mL, (c) 0.05 U/mL, (d) 0.25 U/mL, (e) 0.5 U/mL, (f) 1 U/mL, (g) 5 U/mL, (h) 10 U/mL. (B) Linear relationship for Dam MTase detection between LSV current and the logarithm concentration of target.

Fig. 4. (A) Specificity of the biosensor for Dam MTase detection. (B) Inhibition efficiency of Dam MTase by 5-fluorouracil with concentration range from 0 to 500 μM. (C) Inhibition efficiency of Dam MTase by gentamycin with concentration range from 0 to 2.0 μM.

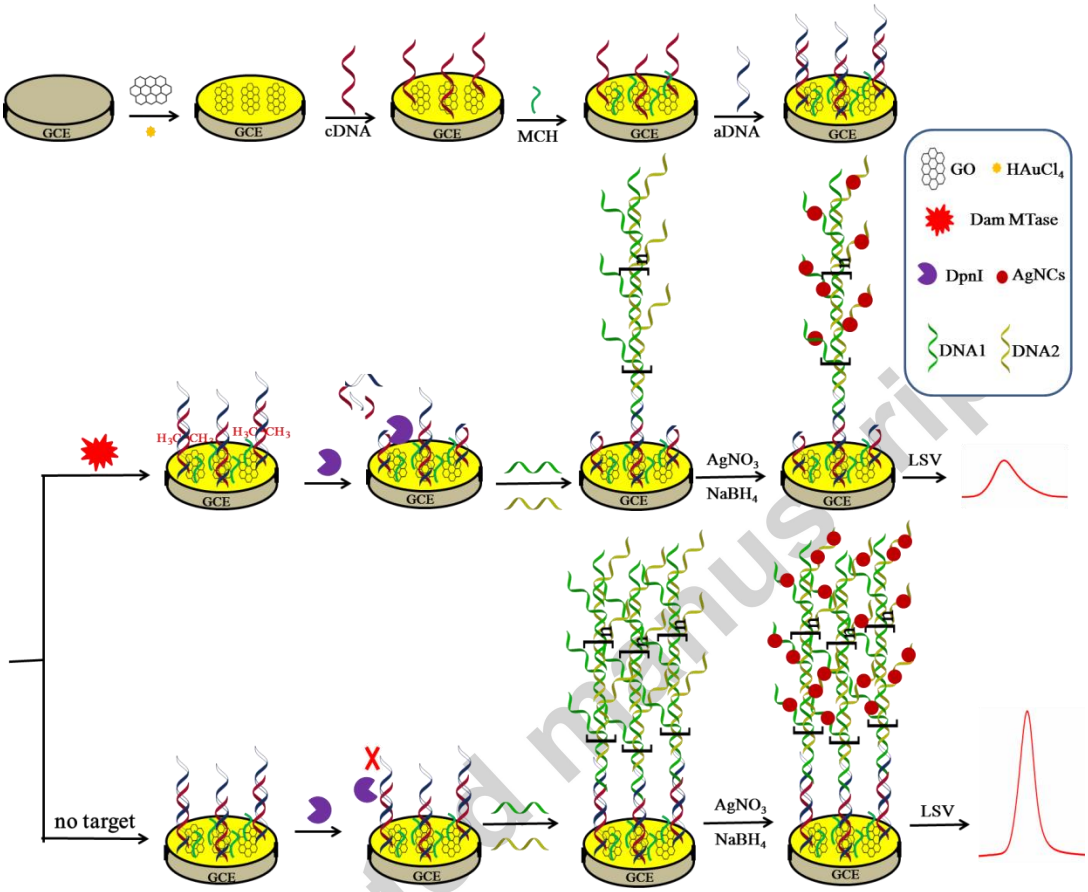

Scheme 1

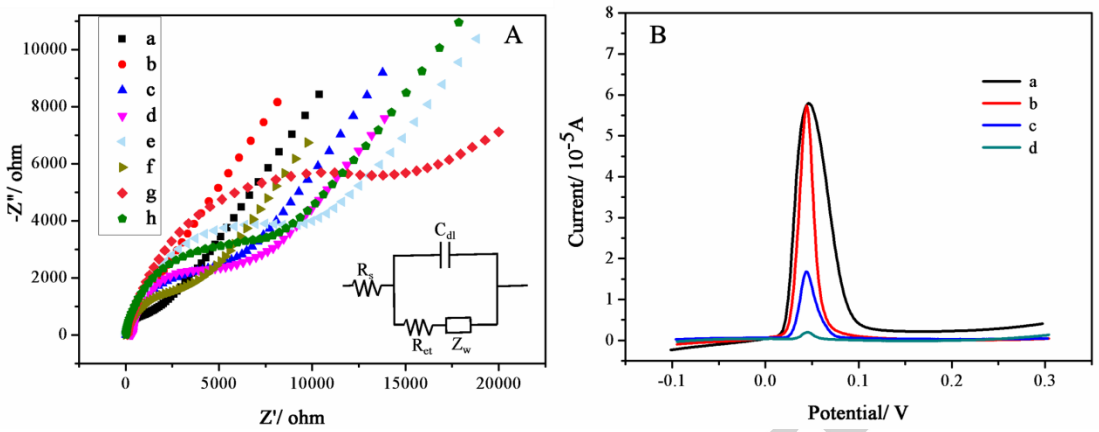

Fig. 1

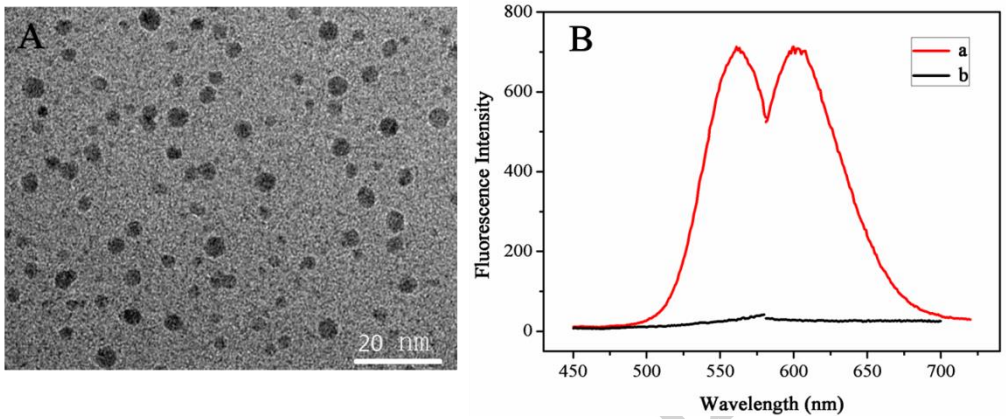

Fig. 2

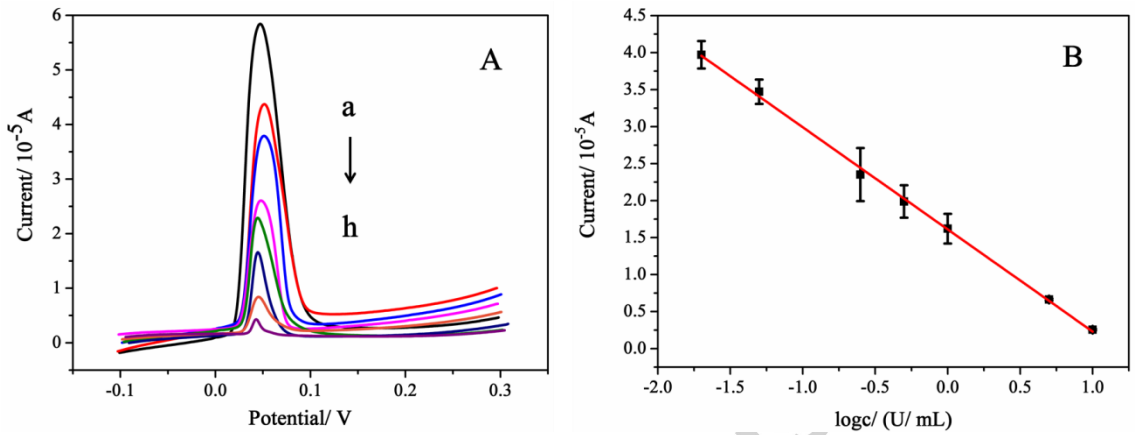

Fig. 3

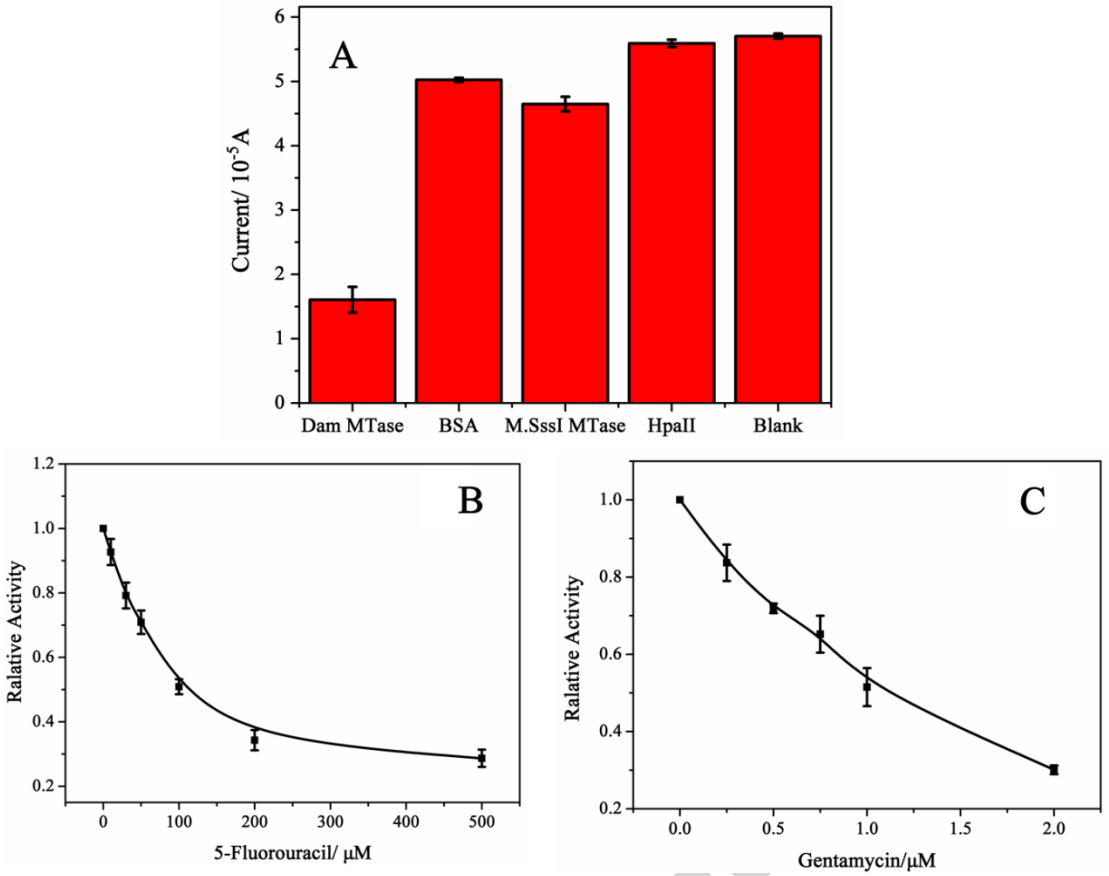

Fig. 4

Table 1. Comparison of different methods for Dam MTase detection.

Detection method	Amplification strategy	Liner range	Detection limit	ref
Fluorescence	Exo III	0-50 U/mL	0.01 U/mL	Xing et al., 2014
Electrochemiluminescence	GO/AgNPs/luminol	0.1-20 U/mL	0.03 U/mL	Zhao et al., 2015
Fluorescence	DNA Tetrahedron	0.1-90 U/mL	0.045 U/mL	Zhou et al., 2017
Fluorescence	HCR	0-1.0 U/mL	0.015 U/mL	Wang et al., 2017
Electrochemical biosensor	AuNPs	0.27-40 U/mL	0.27 U/mL	Liu et al., 2016
Electrochemical biosensor	GQD/HRP	1-40 U/mL	0.3 U/mL	Peng et al., 2017
Electrochemical biosensor	AuNPs/ERGO/HCR/AgNCs	0.02 -10 U/mL	0.0073U/mL	this work

Highlights

1. The proposed biosensor achieved the ultrasensitive detection of Dam MTase and inhibitors screening.
2. The AuNPs/ERGO hybrids and HCR amplification strategy improved the sensitivity of Dam MTase detection.
3. The ds-DNA superstructures formed by HCR process could be as effective template for AgNCs synthesis.
4. The in-situ synthesized AgNCs could be as signal probes to provide amplified current signal output.